Classification of a 3-RER Parallel Manipulator Based on the Type and Number of Operation Modes

Xianwen Kong

School of Engineering and Physical Sciences,
Heriot-Watt University,
Edinburgh EH14 4AS, UK
email: X.Kong@hw.ac.uk

The type/number of operation modes of a parallel manipulator (PM) may vary with the link parameters of the PM. This paper presents a systematic classification of a 3-RER PM based on the type/number of operation modes. Here, R and E denote revolute joint and planar joint, respectively. The 3-RER PM was proposed as a 4-degree-of-freedom (DOF) 3T1R PM in the literature. Using the proposed method, classification of a PM based on the type/number of operation modes can be carried out in four steps, including formulation of constraint equations of the PM, preliminary classification of the PM using Gröbner cover, operation mode analysis of all the types of PMs using primary decomposition of ideals, and identification of redundant types of PMs. The classification of the 3-RER PM shows that it has 13 types. Besides the two 4-DOF 3T1R operation modes, different types of 3-RER PMs may have up to two more 3-DOF or other types of 4-DOF operation modes. Motion characteristics of the moving platform of 3-RER PMs are also identified using Euler parameter quaternions. This work is the first systematic study on the impact of link parameters on the operation modes of the 3-RER PM and provides a solid foundation for further research on the design and control of 3-RER PMs and other multi-mode (or reconfigurable) PMs. [DOI: 10.1115/1.4048262]

Keywords: multi-mode mechanism, operation mode, quaternion, Euler parameters, Gröbner cover

1 Introduction

The impacts of link parameters on the degree of characteristic univariate polynomial equations for the forward kinematics of parallel manipulators (PMs) have been well studied (see for instance Refs. [1–4]). Recently, it has been shown [5–7] that the type/number of operation modes of a PM may vary with the link parameters of the PM. For example, it was revealed in 2012 that there exist variable degree-of-freedom (DOF) PMs with both 4-DOF PPPR equivalent (also 3T1R or Schönflies motion) and 3-DOF E (also planar motion) operation modes [5]. Here and throughout this paper, R, P, U, and E denote revolute joint, prismatic joint, universal joint, and planar joint, respectively. Both the 4-UPU PM with congruent square base and platform [6] and the 3-RER PM with congruent triangular base and platform [7] have two types of 4-DOF operation modes. In addition to the two 4-DOF 3T1R operation modes, there is also a 4-DOF 2R2T zero-torsion mode. The geometric characteristics of the 4-DOF 2R2T operation modes have been revealed in Ref. [7]. All the operation modes of a PM can be obtained using primary decomposition of ideals [8–11], which is an efficient tool for obtaining the positive dimensional solutions to polynomial constraint equations of the PM.

However, except the work in Refs. [5–7] in which the link parameters are set by intuition, no systematic study has been presented on the impact of link parameters on the type/number of operation modes of a PM. Such a systematic study is essential for the design and control of conventional PMs and reconfigurable PMs. Unfortunately, the method for investigating the impact of link parameters on the forward kinematics [1–4] is not applicable to the study on the impact of link parameters on the type/number of

operation modes of a PM, which requires solving high-dimensional parametric polynomial equations.

Significant advances have been made in solving parametric polynomial systems. Since 1992 when Weispfenning proved that any parametric polynomial ideal has a finite comprehensive Gröbner system (CGS) [12], several approaches (see Refs. [13–15] for example) have been proposed for computing CGS for parametric polynomial ideals. Recently, a method based on Gröbner cover [14] was used for the inverse kinematic analysis of planar manipulators, the kinematic analysis of planar mechanisms, and the identification of over-constrained planar mechanisms [16]. The advances in computing CGS or Gröbner cover of parametric polynomial systems provide an efficient tool for the classification of the above 3-RER PM.

Considering the scale of parametric polynomial systems that the current algorithms [13–15] can solve, this paper is to investigate the classification of a 3-RER PM, which was originally proposed as a 3T1R PM [17–19].

A brief introduction to Gröbner cover will be presented in Sec. 2. In Sec. 3, steps for the classifications based on the type/number of operation modes will be proposed. In Sec. 4, the description of the 3-RER PM will be given. The constraint equations of the 3-RER PM will be formulated in Sec. 5. The preliminary classification of the 3-RER PM will be dealt with using Gröbner cover in Sec. 6. The operation mode analysis of different types of 3-RER PMs will be determined using primary decomposition of ideals in Sec. 7. Motion characteristics of the moving platform of 3-RER PMs will also be identified using Euler parameter quaternions. In Sec. 8, redundant types of 3-RER PMs will be identified. Several factors influencing the type/number of operation modes of the 3-RER PM will also be discussed in Sec. 9. Finally, conclusions will be drawn.

2 Gröbner Cover

According to Ref. [13], Wibmer's theorem establishes that for a homogeneous parametric polynomial ideal, there exists a canonical partition of the parameter space into locally closed segments each of which accepts a set of functions that specializes to the reduced

Table 1 Intersections of two lines obtained using Gröbner cover

No	Segments	Intersection
S1	$a \neq 0$	$\begin{cases} y = 0 \\ x = -c/a \end{cases}$
S2	$\begin{cases} a = 0 \\ c \neq 0 \end{cases}$	$x \to \infty$
S3	$\begin{cases} a = 0 \\ c = 0 \end{cases}$	$y = 0$

Fig. 1 A 3-RER PM: (a) CAD model and (b) type representation

Gröbner basis for every point within the segment and each segment has different leading power products (lpps). The library for calculating Gröbner cover in Ref. [14], grobcov.lib, will be used in this paper to obtain the segments and the Gröbner bases associated with these segments.

In the following, the use of Gröbner cover will be illustrated by obtaining the well-known three cases of intersection of two straight lines. For simplicity reasons, let one straight line coincide with the X-axis. The intersection of two straight lines can be expressed using the following set of parametric linear equations

$$\begin{cases} ax + by + c = 0 \\ y = 0 \end{cases} \tag{1}$$

The ideal associated with the set of polynomial equations in Eq. (1) is

$$S = \langle ax + by + c, \, y \rangle$$

Using the following SINGULAR code,[1] we can obtain the Gröbner cover, which shows the three segments in the parametric space (a, b, c) together with the solutions in these segments as shown in Table 1.

```
LIB "grobcov.lib";
ring R=(0,a,b,c),(x,y),dp;
ideal S = y, ax + by + c;
grobcov(S,"showhom",1);
```
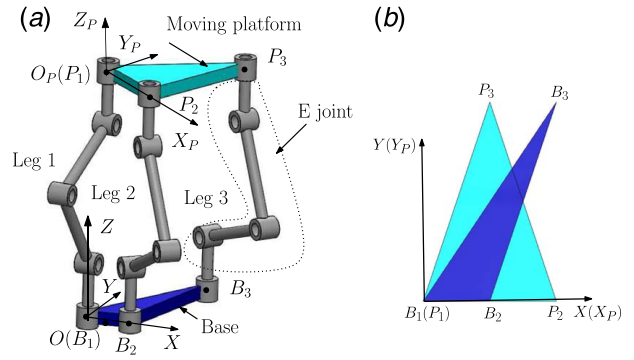
Although the above solutions to Eq. (1) can be easily derived without using a computer, one needs to use the algorithm/library [14] developed recently to calculate the Gröbner cover of more completed parametric polynomial systems.

3 Steps for the Classification of a Parallel Manipulator Based on the Type/number of Operation Modes

Classification of a PM based on the type/number of operation modes can be carried out using the four steps below:

Step 1 Formulation of the constraint equations of the PM.
Step 2 Preliminary classification of the PM using Gröbner cover [14]. Using SINGULAR, we can obtain the Gröbner cover of the ideal associated with the constrained equations obtained in Step 1. For the classification of the PM, we only care about the segments within the Gröbner cover. The Gröbner basis associated with each segment is not critical since it cannot represent the corresponding operation modes clearly. Each real segment is in fact a preliminary type of the PM.
Step 3 Operation mode analysis of all the types of PMs using primary decomposition of ideals. Using the primary decomposition of ideals [8–11], one can calculate the positive dimensional solutions to the polynomial constraint equations

of a PM. Each positive dimensional solution is associated with one operation mode of the PMs. In this step, the operation modes associated with each type of PM are determined using the primary decomposition of ideals.
Step 4 Identification of redundant types of PMs.

4 Description of a 3-RER Parallel Manipulator

A 3-RER PM (Fig. 1(a)) is composed of a moving platform connected to the base by three RER legs. Each RER leg is a serial kinematic chain composed of an R joint, an E joint, and an R joint in sequence. In each leg, the axes of the two R joints are located on the same plane parallel to the plane of motion of the E joint. An E joint is represented by a sub-chain composed of three R joints with parallel axes in this paper. The axes of the R joints on the base (or moving platform) are all parallel. As will be shown in Sec. 7, whether the axes of the R joints on the moving platform are parallel to those on the base largely depends on the operation modes of the PM.

The joint centers, B_i (i=1, 2 and 3), of R joints on the base are the intersections of the joint axes and a plane perpendicular to these axes. The joint centers, P_i (i=1, 2 and 3), of R joints on the moving platform are the intersections of the joint axes and a plane perpendicular to these axes.

Let $O - XYZ$ and $O_P - X_P Y_P Z_P$ denote the coordinate frames fixed on the base and moving platform, respectively. O and O_P are located at B_1 and P_1. The Z- and Z_P-axes are, respectively, parallel to the axes of the three R joints on the base and those on the moving platform. The X- and X_P-axes pass through joint centers B_2 and P_2, respectively. Let $\mathbf{O}_P = \{x \, y \, z\}^T$ represent the position of O_P in the coordinate system $O - XYZ$. The coordinates of B_1, B_2, and B_3 in $O - XYZ$ are $(0, 0, 0)$, $(0, a_1, 0)$, and $(a_2, a_3, 0)$. The coordinates of P_1, P_2, and P_3 in $O_P - X_P Y_P Z_P$ are $(0, 0, 0)$, $(0, b_1, 0)$, and $(b_2, b_3, 0)$. Let $\mathbf{i}$, $\mathbf{j}$, and $\mathbf{k}$ denote the unit vectors along the X-, Y-, and Z-axes, respectively. Let $\mathbf{w_1}$, $\mathbf{w_2}$, and $\mathbf{w_3}$ denote the unit vectors along the X_P-, Y_P-, and Z_P-axes in the coordinate system $O - XYZ$.

As will be shown later in this paper, the number and type of operation modes of the 3-RER PMs depend on the link parameters of the base and platform. Therefore, a type of the 3-RER PM (Fig. 1(b)) can be simply illustrated by the base and moving platform, which are represented by triangles $B_1 B_2 B_3$ and $P_1 P_2 P_3$ formed by the joint centers, in the initial configuration in which $O - XYZ$ and $O_P - X_P Y_P Z_P$ coincide. All the legs are omitted for simplicity reasons.

5 Step 1: Formulation of Constraint Equations of the 3-RER PM

The position vectors of joint centers, B_i, of the three R joints on the base are

$$\begin{cases} \mathbf{r}_{B1} = \mathbf{0} \\ \mathbf{r}_{B2} = a_1 \mathbf{i} \\ \mathbf{r}_{B3} = a_2 \mathbf{i} + a_3 \mathbf{j} \end{cases} \tag{2}$$

---

[1]The degree reverse lexicographical ordering (dp) is used in the analysis of the 3-RER PMs since it is found that the CPU time required is much less than using other options.

The position vectors of joint centers, P_i, of the three R joints on the moving platform are

$$\begin{cases} \mathbf{r}_{P1} = \mathbf{O}_P \\ \mathbf{r}_{P2} = \mathbf{O}_P + b_1\mathbf{w}_1 \\ \mathbf{r}_{P3} = \mathbf{O}_P + b_2\mathbf{w}_1 + b_3\mathbf{w}_2 \end{cases} \qquad (3)$$

In each RER leg, the axes of the two R joints are always coplanar due to the constraint imposed by the E joint, i.e., the triple product of the two unit vectors along the axes of the two R joints of leg i and vector $(\mathbf{r}_{Pi} - \mathbf{r}_{Bi})$ is equal to zero. Then, we obtain the set of constraint equations of leg i (i =1, 2 and 3) as [7]

$$(\mathbf{w}_3 \times \mathbf{k}) \cdot (\mathbf{r}_{Pi} - \mathbf{r}_{Bi}) = 0, \, i = 1, \, 2 \text{ and } 3 \qquad (4)$$

Substituting Eqs. (2) and (3) into Eq. (4), we have

$$\begin{cases} (\mathbf{w}_3 \times \mathbf{k}) \cdot \mathbf{O}_P = 0 \\ (\mathbf{w}_3 \times \mathbf{k}) \cdot (\mathbf{O}_P + b_1\mathbf{w}_1 - a_1\mathbf{i}) = 0 \\ (\mathbf{w}_3 \times \mathbf{k}) \cdot (\mathbf{O}_P + b_2\mathbf{w}_1 + b_3\mathbf{w}_2 - a_2\mathbf{i} - a_3\mathbf{j}) = 0 \end{cases} \qquad (5)$$

Subtracting the second and third equations by the first equation, Eq. (5) becomes

$$\begin{cases} (\mathbf{w}_3 \times \mathbf{k}) \cdot \mathbf{O}_P = 0 \\ (\mathbf{w}_3 \times \mathbf{k}) \cdot (b_1\mathbf{w}_1 - a_1\mathbf{i}) = 0 \\ (\mathbf{w}_3 \times \mathbf{k}) \cdot (b_2\mathbf{w}_1 + b_3\mathbf{w}_2 - a_2\mathbf{i} - a_3\mathbf{j}) = 0 \end{cases} \qquad (6)$$

Using Euler parameters to represent the orientation of the moving platform, the unit vectors along X_P- and Y_P-, and Z_P-axes are [8]

$$\mathbf{w}_1 = \begin{Bmatrix} e_0^2 + e_1^2 - e_2^2 - e_3^2 \\ 2(e_1e_2 + e_0e_3) \\ 2(e_1e_3 - e_0e_2) \end{Bmatrix} \qquad (7)$$

$$\mathbf{w}_2 = \begin{Bmatrix} 2(e_1e_2 - e_0e_3) \\ e_0^2 - e_1^2 + e_2^2 - e_3^2 \\ 2(e_2e_3 + e_0e_1) \end{Bmatrix} \qquad (8)$$

$$\mathbf{w}_3 = \begin{Bmatrix} 2(e_1e_3 + e_0e_2) \\ 2(e_2e_3 - e_0e_1) \\ e_0^2 - e_1^2 - e_2^2 + e_3^2 \end{Bmatrix} \qquad (9)$$

where

$$e_0^2 + e_1^2 + e_2^2 + e_3^2 = 1 \qquad (10)$$

Substituting Eqs. (7)–(9) into Eq. (6), we obtain

$$\begin{cases} (e_0e_1 - e_2e_3)x + y(e_0e_2 + e_1e_3) = 0 \\ -e_1(a_1 - b_1)e_0 + e_2e_3(a_1 + b_1) = 0 \\ ((-a_2 + b_2)e_1 - e_2(a_3 - b_3))e_0 + \\ ((-a_3 - b_3)e_1 + e_2(a_2 + b_2))e_3 = 0 \end{cases} \qquad (11)$$

Equations (10) and (11) are the parametric polynomial equations for the classification and operation mode analysis of the 3-RER PM.

6 Step 2: Preliminary Classification of the 3-RER PM Using Gröbner Cover

Without loss of generality and in order to simplify the computation of Gröbner cover, we can assume

$$a_1 = 1 \qquad (12)$$

Substituting Eq. (12) into Eq. (11), we have

$$\begin{cases} (e_0e_1 - e_2e_3)x + y(e_0e_2 + e_1e_3) = 0 \\ -e_1(1 - b_1)e_0 + e_2e_3(1 + b_1) = 0 \\ ((-a_2 + b_2)e_1 - e_2(a_3 - b_3))e_0 + \\ ((-a_3 - b_3)e_1 + e_2(a_2 + b_2))e_3 = 0 \end{cases} \qquad (13)$$

Using SINGULAR, we can obtain the Gröbner cover [14] of the ideal associated with Eq. (13). For the classification of the 3-RER PM, we only care about the segments within the Gröbner cover. The Gröbner basis associated with each segment cannot represent the corresponding operation modes clearly without applying primary decomposition to it. It is more convenient to identify the operation modes of a given PM by calculating the primary

Table 2   Segments in the parametric space of the 3-RER PM

Segment ID	Segment Definition (True/False)
S1	T: - F: b_3, $a_3 + b_3$, $a_3 - b_3$, b_1, $b_1 - 1$
S2	T: $b_1 - 1$ F: $(b_1 - 1, a_2 - b_2)$, $(b_1 - 1, a_3 + b_3)$, $(b_1 - 1, a_3 - b_3)$
S3	T: $(b_1 - 1, a_2 - b_2)$ F: $(b_1 - 1, a_3 + b_3, a_2 - b_2)$, $(b_1 - 1, a_3 - b_3, a_2 - b_2)$
S4	T: $(b_1 - 1, a_3 - b_3, a_2 - b_2)$ F: $(b_3, b_1 - 1, a_3, a_2 - b_2)$
S5	T: $(b_3, b_1 - 1, a_3, a_2 - b_2)$ F: -
S6	T: $(b_1 - 1, a_3 + b_3, a_2 - b_2)$ F: $(b_3, b_1 - 1, a_3, a_2 - b_2)$
S7	T: $(b_1 - 1, a_3 - b_3)$ F: $(b_3, b_1 - 1, a_3)$, $(b_1 - 1, a_3 - b_3, a_2 - b_2)$
S8	T: (b_3, a_3) F: $(b_3, a_3, a_2b_1 - b_2)$
S9	T: $(b_1 - 1, a_3 + b_3)$ F: $(b_3, b_1 - 1, a_3)$, $(b_1 - 1, a_3 + b_3, a_2 - b_2)$
S10	T: $a_3 - b_3$ F: (b_3, a_3), $(a_3 - b_3, a_2b_1 - b_2)$, $(b_1, a_3 - b_3)$, $(b_1 - 1, a_3 - b_3)$
S11	T: $(b_3, a_3, a_2b_1 - b_2)$ F: $(b_3, b_1 - 1, a_3, a_2 - b_2)$
S12	T: $(a_3 - b_3, a_2b_1 - b_2)$ F: $(b_3, a_3, a_2b_1 - b_2)$, $(b_1 + 1, a_3 - b_3, a_2 + b_2)$, $(b_1 - 1, a_3 - b_3, a_2 - b_2)$
S13	T: $(b_1 + 1, a_3 - b_3, a_2 + b_2)$ F: $(b_3, b_1 + 1, a_3, a_2 + b_2)$
S14	T: $(b_1, a_3 - b_3)$ F: $(b_2, b_1, a_3 - b_3)$, $(b_2^2 + b_3^2, b_1, a_3 - b_3)$, (b_3, b_1, a_3)
(S15)	T: $(b_2^2 + b_3^2, b_1, a_3 - b_3)$ F: (b_3, b_2, b_1, a_3)
S16	T: $a_3 + b_3$ F: (b_3, a_3), $(a_3 + b_3, a_2b_1 - b_2)$, $(b_1, a_3 + b_3)$, $(b_1 - 1, a_3 + b_3)$
S17	T: $(a_3 + b_3, a_2b_1 - b_2)$ F: $(b_3, a_3, a_2b_1 - b_2)$, $(b_1 + 1, a_3 + b_3, a_2 + b_2)$, $(b_1 - 1, a_3 + b_3, a_2 - b_2)$
S18	T: $(b_1 + 1, a_3 + b_3, a_2 + b_2)$ F: $(b_3, b_1 + 1, a_3, a_2 + b_2)$
S19	T: $(b_1, a_3 + b_3)$ F: (b_3, b_1, a_3), $(b_2^2 + b_3^2, b_1, a_3 + b_3)$, $(b_2, b_1, a_3 + b_3)$
(S20)	T: $(b_2^2 + b_3^2, b_1, a_3 + b_3)$ F: (b_3, b_2, b_1, a_3)
S21	T: b_3 F: (b_3, b_1), $(b_3, b_1 - 1)$, (b_3, a_3)
S22	T: (b_3, b_1) F: (b_3, b_2, b_1), (b_3, b_1, a_3)
(S23)	T: (b_3, b_2, b_1) F: (b_3, b_2, b_1, a_3)
S24	T: b_1 F: (b_3, b_1), $(b_2^2 + b_3^2, b_1)$, $(b_1, a_3 + b_3)$, $(b_1, a_3 - b_3)$
(S25)	T: $(b_2^2 + b_3^2, b_1)$ F: (b_3, b_2, b_1), $(b_2^2 + b_3^2, b_1, a_3 + b_3)$, $(b_2^2 + b_3^2, b_1, a_3 - b_3)$

Table 3 Parameters of different types of 3-RER PMs

Type	a_1	a_2	a_3	b_1	b_2	b_3
S1	1	2	3	2	1	4
S2		2	3	1	1	4
S3		2	3	1	2	4
S4		2	3	1	2	3
S5		2	0	1	2	0
S6		2	3	1	2	−3
S7		2	3	1	1	3
S8		2	0	2	1	0
S9		2	3	1	1	−3
S10		2	3	2	1	3
S11		2	0	2	4	0
S12		2	3	2	4	3
S13		2	3	−1	−2	3
S14		2	3	0	1	3
S16		2	3	2	1	−3
S17		2	3	2	4	−3
S18		2	3	−1	−2	−3
S19		2	3	0	1	−3
S21		2	3	2	5	0
S22		2	3	0	$\sqrt{5}$	0
S24		2	3	0	1	2

decomposition of its particular ideal associated with the constraint equations (Eq. (13)).

The segments for the 3-RER PM obtained are listed in Table 2. For simplicity reasons, the notation for representing segments in Ref. [16] is used in this paper. For example, segment S2 in Table 2 is

$$\begin{cases} b_1 - 1 = 0 \\ a_2 - b_2 \neq 0 \\ a_3 + b_3 \neq 0 \\ a_3 - b_3 \neq 0 \end{cases} \quad (14)$$

Among the 25 segments, three segments, including S15, S20, and S25, allow only complex link parameters, and segment S23 leads to a degenerated 3-RER PM. Discarding these four segments by placing their type numbers in brackets in Table 2, the parameter space of the 3-RER PM is divided into 21 segments. Therefore, the 3-RER PM can be classified into 21 types.

7 Step 3: Operation Mode Analysis of 3-RER PMs Using Primary Decomposition of Ideals

For each type of 3-RER PM, all the operation modes can be obtained using the primary decomposition of ideals [8–11]. Table 3 lists the link parameters of different types of 3-RER PMs, the operation modes of which will be presented later in this section.

The analysis shows that all the 21 types of 3-RER PMs have the following two operation modes:

$$\begin{cases} e_1 = 0 \\ e_2 = 0 \end{cases} \quad (15)$$

$$\begin{cases} e_0 = 0 \\ e_3 = 0 \end{cases} \quad (16)$$

The remaining operation modes of 13 out of 21 types of 3-RER PMs, including types S1, S2, S3, S4, S5, S7, S8, S10, S11, S12, S14, S21, and S22, are given in Tables 4–7. As shown in the next section, the other eight types of 3-RER PMs are redundant. It is noted that the example Types S1 and S22 3-RER PMs have no operation mode other than the two operation modes represented by Eqs. (15) and (16).

In each operation mode, the DOF of a 3-RER PM can usually be obtained by calculating the difference between the number of variables (x, y, z, e_0, e_1, e_2, and e_3) and the number of independent constraint equations. For example, the DOF of a 3-RER PM in the operation mode associated with Eqs. (10) and (16) is 4 (=7-3). Two exceptional cases are Type S11 (Table 4) and S21 (Table 5) 3-RER PMs. One can also obtain the DOF of the 3-RER PM

Table 4 Operation modes of the 3-RER PMs except the two 3T1R modes: PMs with collinear base and platform

Type	Kinematic diagram	Operation mode	Description
S5		$\begin{cases} e_0 x + e_3 y = 0 \\ e_2 = 0 \end{cases}$	4-DOF 2T2R motion: Half-turn rotation about the Y-axis followed by a half-turn rotation about the axis $\mathbf{u} = \{e_3 - e_0 - e_1\}^T$ and subsequent 2-DOF translation perpendicular to $\{e_0\ e_3\ 0\}^T$.
		$\begin{cases} e_1 x + e_2 y = 0 \\ e_3 = 0 \end{cases}$	4-DOF 2T2R motion: Half-turn rotation about the Z-axis followed by a half-turn rotation about the axis $\mathbf{u} = \{-e_2\ e_1 - e_0\}^T$ and subsequent 2-DOF translation perpendicular to $\{e_1\ e_2\ 0\}^T$.
S11		$\begin{cases} e_0^2 y - 4 e_0 e_3 x - 3 e_3^2 y = 0 \\ e_0 e_1 + 3 e_2 e_3 = 0 \\ e_0 e_2 y + e_1 e_3 y - 4 e_2 e_3 x = 0 \\ e_1^2 y - 4 e_1 e_2 x - 3 e_2^2 y = 0 \end{cases}$	4-DOF 2T2R motion
S8		$\begin{cases} e_0 = 0 \\ e_2 = 0 \\ y = 0 \end{cases}$	Half-turn rotation about the Z-axis followed by 3-DOF planar motion along the $O - XZ$ plane
		$\begin{cases} e_1 = 0 \\ e_3 = 0 \\ y = 0 \end{cases}$	3-DOF planar motion along the $O - XZ$ plane

Table 5 Operation modes of the 3-RER PMs except the two 3T1R modes: PMs with a collinear platform

Type	Kinematic diagram	Operation mode	Description
S14		$\begin{cases} e_0 - 3e_3 = 0 \\ 3e_1 - e_2 = 0 \\ y = 0 \end{cases}$	Rotation about the Z-axis by $2atan2(1, 3)$ followed by 3-DOF motion along the $O - XZ$ plane
		$\begin{cases} e_1 = 0 \\ e_3 = 0 \\ y = 0 \end{cases}$	3-DOF planar motion along the $O - XZ$ plane
S21		$\begin{cases} 3e_0^2 + 2e_0 e_3 - 9e_3^2 = 0 \\ e_0 e_1 + 3e_2 e_3 = 0 \\ 3e_0 e_2 + 3e_1 e_3 + 2e_2 e_3 = 0 \\ 3e_1^2 + 2e_1 e_2 - 9e_2^2 = 0 \\ 6x + y = 0 \end{cases}$	Rotation about the Z-axis by $2atan2(-3, 1 + 2\sqrt{7})$ (or by $2atan2(3, -1 + 2\sqrt{7})$) followed by 3-DOF planar motion along plane $6x + y = 0$
S22		–	–

with a set of complicated constraint equations by calculating the Hilbert dimension of the ideal associated with the constraint equations using a computer algebra system. Using this approach, we can obtain the correct DOF of Type S11 and S21 3-RER PMs.

Using the kinematic interpretation of 15 cases of Euler parameter quaternions [8], the motion characteristics of the moving platform of the PM in most of the operation modes can be readily obtained. For example, the motion represented by Eq. (15) is a 4-DOF 3T1R motion, i.e., rotation by $2atan2(e_3, e_0)$ about the Z-axis followed by 3-DOF spatial translation [7] (Fig. 2(a)). Equation (16) represents a 4-DOF (inverted) 3T1R motion, i.e., half-turn rotation about the X-axis followed by a rotation by $2atan2(e_2, e_1)$ about the Z-axis (or half-turn rotation about the Y-axis followed by a rotation by $2atan2(-e_1, e_2)$ about the Z-axis) and subsequent 3-DOF spatial translation (Fig. 2(b)). At a regular configuration of the 3-RER PM in these two operation modes, all the axes of the R joints on both the base and the moving platform are parallel (Figs. 2(a) and 2(b)).

Types S8, S14, S7, S10, and S12 3-RER PMs have the following 3-DOF operation modes,

$$\begin{cases} e_1 = 0 \\ e_3 = 0 \\ y = 0 \end{cases} \quad (17)$$

Using the kinematic interpretation of Case 6 of Euler parameter quaternions [8], one can obtain that Eq. (17) represents 3-DOF planar motion along the $O - XZ$ plane (Fig. 2(c)). In this 3-DOF planar operation mode, all the E joints are parallel to the $O - XZ$ plane, and the axes of R joints on the moving platform are not always parallel to those on the base.

The kinematic interpretation of motion of several 3-RER PMs in a 3-DOF operation mode, such as Type S10 3-RER PM in the operation mode shown in Eq. (18), cannot be obtained using the kinematic interpretation of 15 specific cases of Euler parameter quaternions [8].

$$\begin{cases} e_0 + 3e_3 = 0 \\ e_1 - e_2 = 0 \\ 2x + y = 0 \end{cases} \quad (18)$$

It is noted that in all the constraint equations of a 3-RER PM at a 3-DOF operation mode (Tables 4–7), each constraint equation is either in (a) e_0, e_1, e_2 and e_3 or in (b) x and y. In addition, there is one constraint equation in x and y. Therefore, the 3-RER PM has two translational DOF and one rotational DOF. The challenge is to identify the kinematic interpretation of the 1-DOF rotation.

Let us take the above 3-DOF operation mode of Type S10 3-RER PM as an example to illustrate how to obtain the interpretation of the 1-DOF rotation and the 3-DOF motion. First, calculate the orientation of the common configuration between the 3T1R operation mode (Eq. (15)) and the 3-DOF operation mode (Eq. (18)). The orientation can be obtained by solving a set of equations composed of Eqs. (10), (15), and (18) as

$$\begin{cases} e_0^2 + e_1^2 + e_2^2 + e_3^2 = 1 \\ e_0 + 3e_3 = 0 \\ e_1 = 0 \\ e_2 = 0 \end{cases} \quad (19)$$
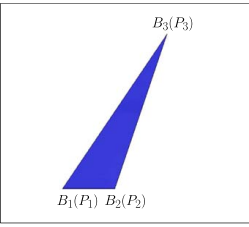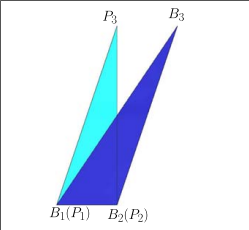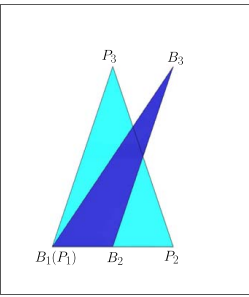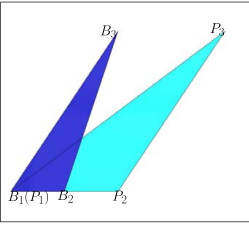
i.e.,

$$\begin{cases} e_3 = -1/\sqrt{10} \\ e_0 = 3/\sqrt{10} \\ e_1 = 0 \\ e_2 = 0 \end{cases} \quad (20)$$

Equation (20) represents a configuration obtained by a rotation about the Z-axis by $2atan2(-1, 3)$. Considering the characteristics of RER leg, we can assume that the 1-DOF rotation in the 3-DOF operation mode of Type S10 is a rotation about the Z-axis by $2atan2(-1, 3)$ followed by a rotation about the normal to plane $2x + y = 0$ by θ. The Euler parameters representing the above

Table 6 Operation modes of the 3-RER PM except the two 3T1R modes: PMs with $b_3 = a_3$

Type	Kinematic diagram	Operation mode	Description
S4		$\begin{cases} e_1 x + e_2 y = 0 \\ e_3 = 0 \end{cases}$	4-DOF 2T2R motion: Half-turn rotation about the Z-axis followed by a half-turn rotation about the axis $\mathbf{u} = \{-e_2 \; e_1 \; -e_0\}^T$ and subsequent 2-DOF translation perpendicular to $\{e_1 \; e_2 \; 0\}^T$.
S7		$\begin{cases} e_0 + 6e_3 = 0 \\ e_2 = 0 \\ 6x - y = 0 \end{cases}$	Rotation about the Z-axis by $2atan2(-1, 6)$ followed by 3-DOF planar motion along plane $6x - y = 0$
		$\begin{cases} e_1 = 0 \\ e_3 = 0 \\ y = 0 \end{cases}$	3-DOF planar motion along the $O - XZ$ plane
S10		$\begin{cases} e_0 + 3e_3 = 0 \\ e_1 - e_2 = 0 \\ 2x + y = 0 \end{cases}$	Rotation about the Z-axis by $2atan2(-1, 3)$ followed by 3-DOF motion along plane $2x + y = 0$
		$\begin{cases} e_1 = 0 \\ e_3 = 0 \\ y = 0 \end{cases}$	3-DOF planar motion along the $O - XZ$ plane
S12		$\begin{cases} e_1 = 0 \\ e_3 = 0 \\ y = 0 \end{cases}$	3-DOF planar motion along the $O - XZ$ plane

motion can be derived as (see the Appendix for details)

$$\begin{cases} e_0 = 3\cos(\theta/2)/\sqrt{10} \\ e_1 = \sin(\theta/2)/\sqrt{2} \\ e_2 = \sin(\theta/2)/\sqrt{2} \\ e_3 = -\cos(\theta/2)/\sqrt{10} \end{cases} \qquad (21)$$

One can verify that the Euler parameters in Eq. (21) meet Eq. (18). This confirms that the above assumption is correct. Therefore, the 1-DOF rotation in this operation mode is a rotation about the Z-axis by $2atan2(-1, 3)$ followed by a rotation about the normal to plane $2x + y = 0$, and the 3-DOF motion is a rotation about the Z-axis by $2atan2(-1, 3)$ followed by a 3-DOF planar motion along plane $2x + y = 0$ (Fig. 2(d)).

The kinematic interpretation of all the types of 3-RER except the 4-DOF 2T2R operation mode of Type S11 PM has been obtained as given in the last column in Tables 4–7. The motion characteristics of Type S11 PM in the 4-DOF 2T2R operation mode needs further investigation.

A type S14, S7, S10, or S2 3-RER PM has two 3-DOF operation modes in which the planes of motion in both operation modes are

different. A type S21 3-RER PM (Table 4) has two 3-DOF operation modes along the same plane but the moving platform has different orientations (Fig. 3).
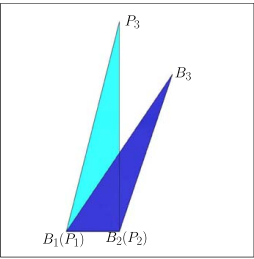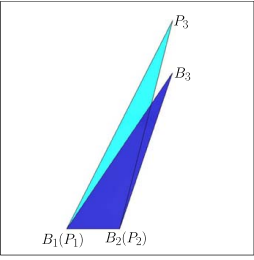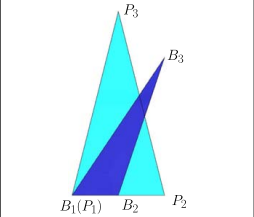
Tables 4–7 show that all the 3-DOF operation modes of any 3-RER PMs are 3-DOF planar operation modes. In a 3-DOF planar operation mode, all the E joints of a PM are parallel, and the axes of R joints on the moving platform are not always parallel to those on the base (Figs. 2(c), 2(d), and 3).
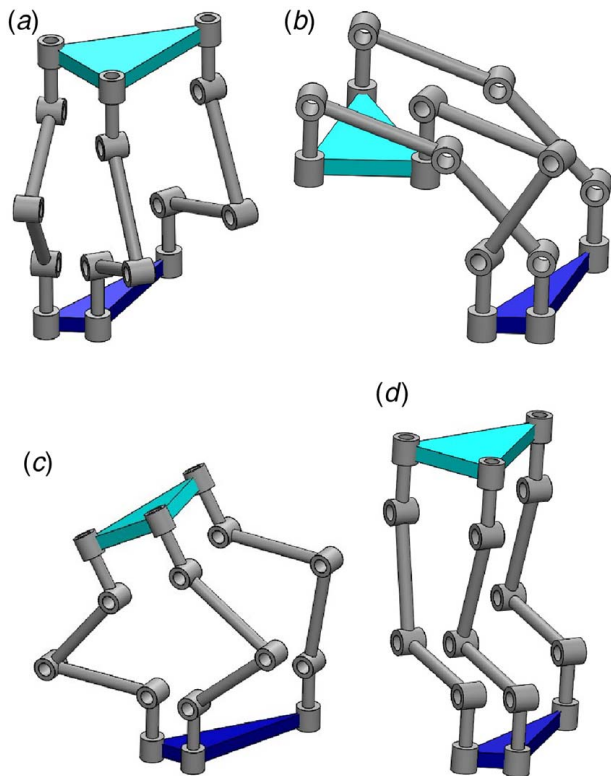
8 Step 4: Identification of Redundant Types of 3-RER PMs

If more than one type of the 21 types of 3-RER PMs can realize the same motion, one type is kept while the other types are called redundant types.

Two types of 3-RER PMs are the same if one type can reach a configuration of another type starting from its initial configuration through motion in the 3T1R operation mode (Eq. (15)) or inverted 3T1R operation mode (Eq. (16)).
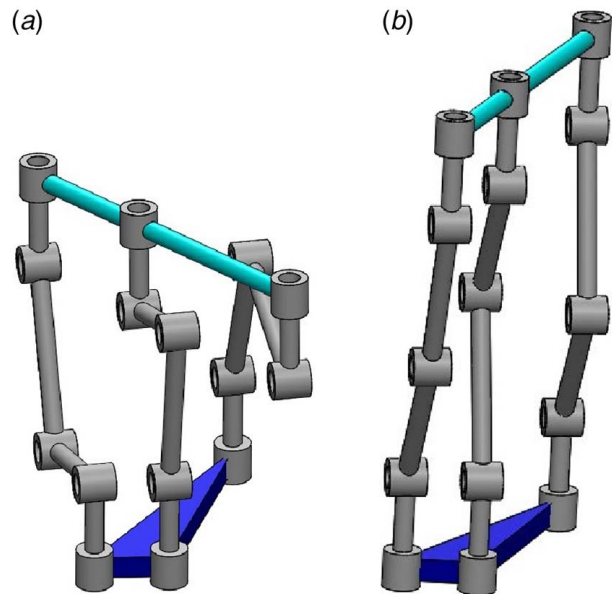
Table 7 Operation modes of the 3-RER PM except the two 3T1R modes: general cases

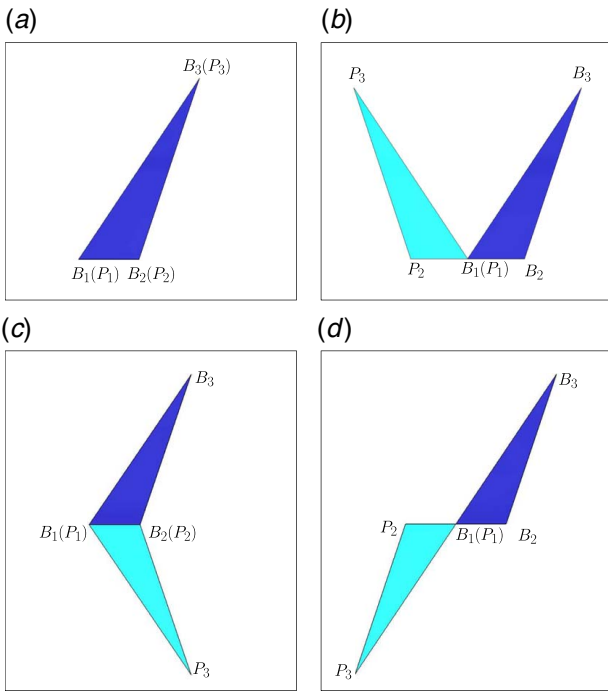| Type	Kinematic diagram	Operation mode	Description
S2		$\begin{cases} e_0 + 7e_3 = 0 \\ e_2 = 0 \\ 7x - y = 0 \end{cases}$	Rotation about the Z-axis by $2atan2(-1, 7)$ followed by 3-DOF planar motion along plane $7x - y = 0$
		$\begin{cases} e_1 - e_2 = 0 \\ e_3 = 0 \\ x + y = 0 \end{cases}$	3-DOF planar motion along plane $x + y = 0$
S3		$\begin{cases} e_2 = 0 \\ e_3 = 0 \\ x = 0 \end{cases}$	3-DOF planar motion along the $O - YZ$ plane
S1		–	–

Fig. 2 Four operation modes of a type S10 3-RER PM: (*a*) 4-DOF 3T1R operation mode 1, (*b*) 4-DOF 3T1R operation mode 2, (*c*) 3-DOF operation mode 1, and (*d*) 3-DOF operation mode 2

Starting from the initial configuration, a type S13 PM (Fig. 4(*b*)) can reach the initial configuration of a type S4 PM (Fig. 4(*a*)) by rotating the moving platform about the *Y*-axis by 180 deg. Starting from the initial configuration, a type S6 (Fig. 4(*c*)) PM can reach the initial configuration of a type S4 PM (Fig. 4(*a*)) by rotating

Fig. 3 Two 3-DOF planar operation modes of a type S21 3-RER PM: (*a*) 3-DOF planar operation mode I and (*b*) 3-DOF planar operation mode II

Fig. 4 Identification of redundant types of 3-RER PMs: (a) type S4, (b) type S13, (c) type S6, and (d) type S18

the moving platform about the Y-axis by 180 deg. Starting from the initial configuration, a type S18 (Fig. 4(d)) PM can reach the initial configuration of a type S4 PM (Fig. 4(a)) by rotating the moving platform about the Z-axis by 180 deg. Therefore, types S4, S6, S13, and S18 3-RER PMs are the same. Type S4 PM is kept while types S6, S13, and S18 PMs are redundant.

Similarly, types S9, S16, S17, S19, and S24 3-RER PMs (Table 3) are redundant since they are the same as types S7, S10, S12, S14, and S22 3-RER PMs, respectively (Table 3).

In addition, type S22 of 3-RER PM must be limited to $b_2 < a_3$ since starting from the initial configuration of a type S22 3-RER PM with $b_2 \geq a_3$, the PM can reach the initial configuration of type S14 by rotating the moving platform about the Z-axis by $arcsin(a_3/b_2)$.

By removing the above eight redundant types of 3-RER PMs, S6, S9, S13, S16, S17, S18, S19, and S24, we obtain 13 types of 3-RER PMs, including three types of PMs with collinear base and platform (types S5, S11, and S8 in Table 4), three types of PMs with collinear platform (types S14, S21, and S22 in Table 5), four types of PMs with $b_3 = a_3$ (types S4, S7, S10, and S12 in Table 6), and three types of PMs of general case (types S2, S3, and S1 in Table 7),

9 Discussion

Based on the observation of the operation modes of the above 13 types of PMs, the main impact of the link parameters on the types/numbers of operation modes of the 3-RER PMs is given below.

(1) A 3-RER PM with congruent base and platform (Type S4) has two 4-DOF 3T1R and one 4-DOF 2T2R operation modes but has no 3-DOF operation modes.
(2) A 3-RER PM with congruent collinear base and platform (Type S5) has two 4-DOF 3T1R and two 4-DOF 2T2R operation modes but has no 3-DOF operation modes.
(3) A 3-RER PM with similar collinear base and platform (type S11) has three 4-DOF operation modes (Table 4).
(4) 3-RER PMs with $a_3 = b_3$ (types S7, S10, S12, and S14) and the 3-RER PM with general collinear base and moving platform (type S8) have two 3-DOF planar operation modes along the O-XZ plane.

(5) A 3-RER PM with $b_1 = a_1$ and $b_2 = a_2$ (type S3 in Table 7) has a 3-DOF planar operation mode along the O-YZ plane.

It is noted that both the example types S1 and S22 3-RER PMs have only two 4-DOF 3T1R operation modes represented by Eqs. (15) and (16) and are overconstrained. It is still open to identify the general conditions for such 3-RER PMs with only two 3T1R operation modes and to identify the redundant types automatically.

10 Conclusions

The 3-RER PM has been classified into 13 types using the Gröbner cover and primary decomposition of ideals. The operation mode analysis has shown that besides the two DOF 3T1R operation modes, a 3-RER PM may have up to two more 3-DOF or other types of 4-DOF operation modes depending the type of the PM. Several factors influencing the type/number of operation modes of the 3-RER PM have been identified. Euler parameter quaternions have been found to be very useful for identifying the motion characteristics of the moving platform of 3-RER PMs. It is still open to identify the general conditions for a 3-RER PM to have only two 4-DOF 3T1R operation modes and to eliminate redundant types automatically.

This work is a step forward in the design and control of the 3-RER PM and the classification of n-RER PMs ($n > 3$) and contributes to the study on multi-mode (or reconfigurable) PMs.

Acknowledgment

Conflict of Interest

There are no conflicts of interest.
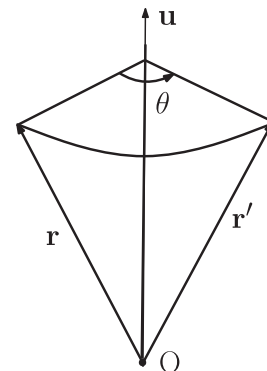
Data Availability Statement

The datasets generated and supporting the findings of this article are obtainable from the corresponding author upon reasonable request. The authors attest that all data for this study are included in the paper.

Appendix: Derivation of Equation (21)

In this appendix, we will derive Eq. (21) using Euler parameter quaternions.

The Euler parameter quaternion (see Ref. [8] for example) is defined as (Fig. 5)

$$q = e_0 + e_1\mathbf{i} + e_2\mathbf{j} + e_3\mathbf{k} = \cos(\theta/2) + \mathbf{u}\sin(\theta/2) \qquad (A1)$$

Fig. 5 Rotation by θ about axis u

where **u** and θ represent, respectively, the axis and angle of rotation. The Euler parameters satisfy Eq. (10).

The product of two Euler parameter quaternions satisfies the following rules:

$$\mathbf{i}^2 = \mathbf{j}^2 = \mathbf{k}^2 = \mathbf{ijk} = -1$$
$$\mathbf{ij} = \mathbf{k} = -\mathbf{ji}$$
$$\mathbf{jk} = \mathbf{i} = -\mathbf{kj} \qquad (A2)$$
$$\mathbf{ki} = \mathbf{j} = -\mathbf{ik}$$

The compositional rotation composed of rotation q_1 followed by rotation q_2 can be represented using the following quaternion:

$$q = q_2 q_1 \qquad (A3)$$

The quaternion representing the rotation about the Z-axis by $2atan2(-1, 3)$ is

$$q_1 = 3/\sqrt{10} - (1/\sqrt{10})\mathbf{k} \qquad (A4)$$

The normal to plane $2x + y = 0$ is $\mathbf{u} = (2/\sqrt{5})\mathbf{i} + (1/\sqrt{5})\mathbf{j}$. The quaternion representing the rotation about **u** by θ is

$$q_2 = \cos(\theta/2) + \sin(\theta/2)[(2/\sqrt{5})\mathbf{i} + (1/\sqrt{5})\mathbf{j}] \qquad (A5)$$

Substituting Eqs. (A4) and (A5) into Eq. (A3), one obtains the quaternion representing the rotation about the Z-axis by $2atan2(-1, 3)$ followed by the rotation about the normal to plane $2x + y = 0$ by θ as

$$q = q_2 q_1 = 3\cos(\theta/2)/\sqrt{10} + (\sin(\theta/2)/\sqrt{2})\mathbf{i}$$
$$+ (\sin(\theta/2)/\sqrt{2})\mathbf{j} - (\cos(\theta/2)/\sqrt{10})\mathbf{k} \qquad (A6)$$

Comparing Eqs. (A1) and (A6), one can obtain Eq. (21).

References

[1] Gosselin, C. M., and Merlet, J-P, 1994, "On the Direct Kinematics of Planar Parallel Manipulators: Special Architectures and Number of Solutions," Mech. Mach. Theory, **29**(8), pp. 1083–1097.

[2] Kong, X., and Yang, T.-L., 1996, "Dimensional Type Synthesis and Special Configuration Analysis of Analytical 6-SPS Parallel Robots," Hi-Tech Lett., **1**(6), pp. 17–20 (in Chinese).

[3] Wenger, P., and Chablat, D., 2009, "Kinematic Analysis of a Class of Analytic Planar 3-RPR Parallel Manipulators," Computational Kinematics, Kecskeméthy, A., Müller, A., eds., Springer, Berlin, Germany, pp. 43–50.

[4] Rojas, N., and Thomas, F., 2011, "The Forward Kinematics of 3-RPR Planar Robots: A Review and a Distance-based Formulation," IEEE Trans. Robot., **27**(1), pp. 143–150.

[5] Kong, X., 2012, "Type Synthesis of Variable Degree-of-Freedom Parallel Manipulators with Both Planar and 3T1R Operation Modes," Proceedings of the IDETC/CIE, Chicago, IL, Aug. 12–15, 2012, ASME Paper No. DETC2012-70621, pp. 497–504.

[6] Coste, M., and Mady Demdah, K., 2015, "Extra Modes of Operation and Self-Motions in Manipulators Designed for Schoenflies Motion," J. Mech. Robot., **7**(4), pp. 041020-041020-6.

[7] Kong, X., 2016, "Reconfiguration Analysis of a 4-DOF 3-RER Parallel Manipulator with Equilateral Triangular Base and Moving Platform," Mech. Mach. Theory., **98**, pp. 180–189.

[8] Kong, X., 2014, "Reconfiguration Analysis of a 3-DOF Parallel Mechanism Using Euler Parameter Quaternions and Algebraic Geometry Method," Mech. Mach. Theory., **74**, pp. 188–201.

[9] Husty, M., and Schröcker, H.-P., 2013, "Kinematics and Algebraic Geometry," 21st Century Kinematics, McCarthy, J.M., eds., Springer, London, UK, pp. 85–123.

[10] Nurahmi, L., Caro, S., Wenger, Ph., Schadlbauer, J., and Husty, M., 2016, "Reconfiguration Analysis of a 4-RUU Parallel Manipulator," Mech. Mach. Theory., **96**, pp. 269–289.

[11] Kong, X., Yu, J., and Li, D., 2016, "Reconfiguration Analysis of a Two Degrees-of-Freedom 3-4R Parallel Manipulator With Planar Base and Platform," ASME J. Mech. Rob., **8**(1), p. 011019.

[12] Weispfenning, V., 1992, "Comprehensive Gröbner Bases," J. Symbol. Comput., **14**(1), pp. 1–29.

[13] Montes, A., and Wibmer, M., 2010, "Gröbner Bases for Polynomial Systems With Parameters," J. Symbol. Comput., **45**(12), pp. 1391–1425.

[14] Montes, A., and Wibmer, M., 2014, "Software for Discussing Parametric Polynomial Systems: The Gröbner Cover," Mathematical Software – ICMS, Hong, H., Yap, C., eds., Springer, Berlin Germany, pp. 406–413.

[15] Hashemi, A., and Darmian, M., 2017, "Computing Comprehensive Gröbner Systems: A Comparison of Two Methods," Comput. Sci. J. Moldova, **25**(3), pp. 278–302.

[16] Arikawa, K., 2019, "Kinematic Analysis of Mechanisms Based on Parametric Polynomial System: Basic Concept of a Method Using Göbner Cover and Its Application to Planar Mechanisms," ASME J. Mech. Rob., **11**(2), p. 020906.

[17] Huang, Z., Li, Q., and Ding, H., 2012, Theory of Parallel Mechanisms, Springer, Dordrecht, The Netherlands.

[18] Yang, T.-L., Liu, A., Shen, H., Hang, L., Luo, Y., and Jin, Q., 2018, Topology Design of Robot Mechanisms, Springer, Singapore.

[19] Kong, X., and Gosselin, C., 2007, Type Synthesis of Parallel Mechanisms, Springer, Dordrecht, The Netherlands.